Surg Radiol Anat (2015) 37:75–80
DOI 10.1007/s00276-014-1321-7

ORIGINAL ARTICLE

The superior ophthalmic vein: delineation with high-resolution magnetic resonance imaging

Satoshi Tsutsumi · Masanobu Nakamura · Takashi Tabuchi · Yukimasa Yasumoto

Received: 29 September 2013 / Accepted: 2 June 2014 / Published online: 15 June 2014

Abstract
Objective To delineate the superior ophthalmic vein (SOV) with high-resolution magnetic resonance (MR) imaging.
Methods This retrospective study enrolled 302 consecutive outpatients, 101 patients, 51 males and 50 females, who underwent coronal T2-weighted imaging and 201 patients, 99 males and 102 females, who underwent three-dimensional (3D) phase-contrast (PC) MR angiography.
Results Coronal T2-weighted imaging clearly delineated the intraorbital course of SOV on serial images in all 101 subjects. The SOV could be topographically divided into three segments in relation to the superior rectus muscle. The SOV crossed over the optic nerve at the level of the anterior ethmoidal foramina in 87 % of right orbits and 71 % of left orbits. The mean outer diameter of the SOV at the crossing point was 1.7 mm on both sides, but the SOVs were asymmetric in the same individual in 75 % of the subjects. 3D PC MR angiography showed that the bilateral SOVs were symmetrical in 16 % of subjects, larger in the right orbit in 18 %, and larger in the left orbit in 13 %, and were unidentified in 52 %. The SOV showed a consistent lateral course to the ophthalmic artery.
Conclusions The SOV consistently courses lateral to the ophthalmic artery, but tends to show bilateral asymmetry in the outer diameter. The superior rectus muscle, anterior ethmoidal foramen, and anterior ethmoidal artery are valuable landmarks to identify the SOV during transcranial orbital surgery. Combination of high-resolution MR imaging and 3D PC MR angiography is useful for delineating the SOV.

Keywords Superior ophthalmic vein · Anatomy · Magnetic resonance imaging · Phase-contrast technique

S. Tsutsumi (✉) · Y. Yasumoto
Department of Neurological Surgery, Juntendo University Urayasu Hospital, 2-1-1 Tomioka, Urayasu, Chiba 279-0021, Japan
e-mail: shotaro@juntendo-urayasu.jp

M. Nakamura · T. Tabuchi
Division of Radiological Technology, Medical Satellite Yaesu Clinic, Tokyo, Japan

Introduction

The superior ophthalmic vein (SOV) is the largest venous structure in the orbit and commonly originates from the junction of two major cutaneous veins, the supraorbital and angular veins. The junction site is situated approximately 4−5 mm behind the tendon of the superior oblique muscle (SObM). The SOV then runs posteriorly and laterally to the SObM, crossing the anterior portion of the optic nerve (ON). More distally, the SOV is joined by the inferior ophthalmic vein and passes through the narrow lateral part of the superior orbital fissure (SOF) together with the trochlear, frontal, and lacrimal nerves. Finally, the SOV drains into the cavernous sinus (Fig. 1) [5, 10, 13]. The SOV has been divided from proximal to distal into the first (SI), second (SII), and third (SIII) segments. The SI is extraconal, whereas the SII and SIII are intraconal [5].

Neuroimaging of the SOV has been mainly described in association with the treatment of various pathological conditions such as carotid-cavernous sinus fistula [7, 8, 13, 17, 22], dural arteriovenous fistula [3], intracranial hypertension [9, 14] and hypotension [4], parasellar tumor [16], and Tolosa−Hunt syndrome [21]. The SOV in the absence of abnormal pathology has been infrequently investigated by computed tomography (CT) [1], three-dimensional (3D) phase-contrast (PC) magnetic resonance (MR) venography

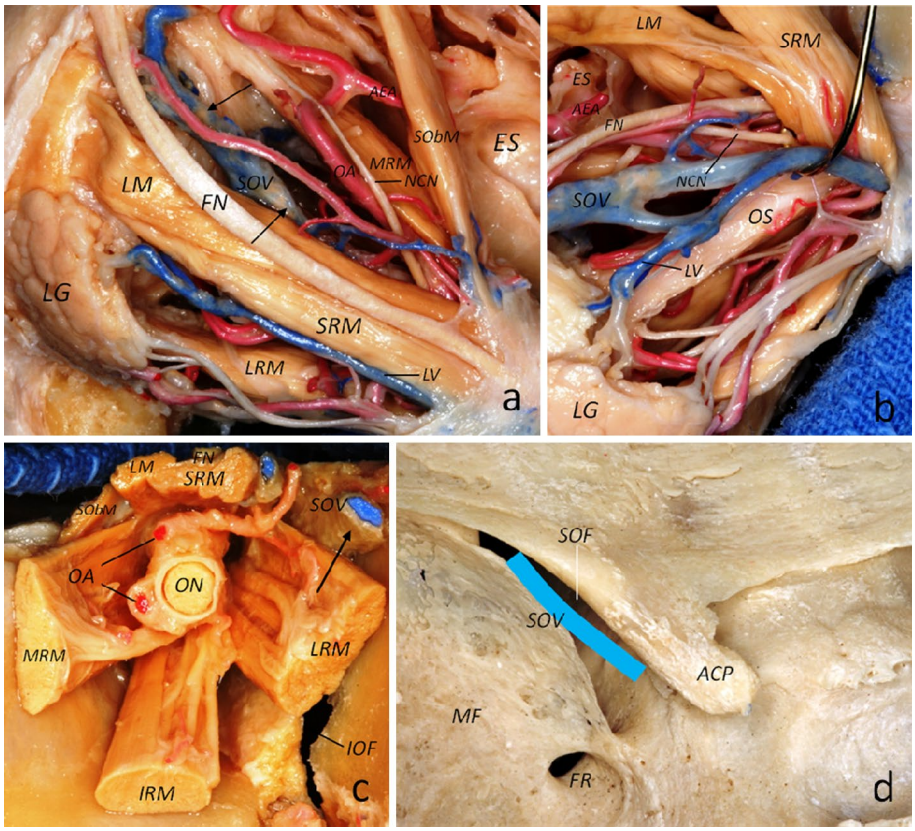

Fig. 1 Cadaveric specimens of the left orbit (**a**–**c**) and dried skull (**d**) demonstrating the intraconal portion of the superior ophthalmic vein (SOV) coursing below the superior rectus muscle on the medial to lateral aspect and crossing over the optic sheath (**a**, **b**, *arrows*), the extraconal segment at the orbital apex coursing between the superior rectus muscle and lateral rectus muscle toward the superior orbital fissure (SOF) (**c**, *arrow*), and the intracranial extraorbital portion emerging from the superolateral part of the SOF connecting to the superolateral portion of the cavernous sinus (**d**). Dissections were performed by the corresponding author at the Department of Neurological Surgery, University of Florida, USA, in 2006. **a**, **d** Posterolateral and superior views. **b** Anterolateral and superior view. **c** Coronal view. *ACP* Anterior clinoid process, *AEA* Anterior ethmoidal artery, *ES* Ethmoid sinus, *FN* Frontal nerve, *FR* Foramen rotundum, *IOF* Inferior orbital fissure, *IRM* Inferior rectus muscle, *LG* Lacrimal gland, *LM* Levator palpebral muscle, *LRM* Lateral rectus muscle, *LV* Lacrimal vein, *MF* Middle fossa, *MRM* Medial rectus muscle, *NCN* Nasociliary nerve, *OA* Ophthalmic artery, *OS* Optic sheath, *SObM* Superior oblique muscle, *SRM* Superior rectus muscle

[6], carotid angiography [15], and orbital phlebography [2], whereas other neuroimaging evaluations of the orbital vasculature did not highlight the SOV [18, 19]. The anatomy of the SOV has not been extensively investigated using high-resolution MR imaging and PC MR angiography.

The present study attempted to delineate the SOV with a combination of high-resolution MR imaging and 3D PC MR angiography.

Materials and methods

This retrospective study included 302 outpatients who underwent MR imaging during February 2009 and September 2013 for headache, vertigo, double vision, syncope, seizure, tinnitus, transient ischemic attack, lacunar infarcts, surveillance study for totally resected brain tumors, and brain check-up. Patients with orbital and cavernous sinus lesions, dural sinus thrombosis, and dural arteriovenous fistula diagnosed by the MR imaging examination, and patients with symptoms of increased intracranial pressure or intracranial hypotension were excluded. The present study was approved by the Medical Satellite Yaesu Clinic Ethics Committee, and written informed consent was obtained from all patients for imaging study, not for the present investigation, according to the Declaration of Helsinki.

All neuroimaging examinations were performed with a 3.0 T MR scanner (Achieva R2.6; Philips Medical Systems, Best, The Netherlands). Coronal T2-weighted imaging was performed in 101 patients using a 32-channel head coil (Achieva R2.6) that involved the whole course of SOV. The parameters were as follows: repetition time (TR) 4,038.35 ms, echo time (TE) 90.00 ms, slice thickness 2.00 mm, interslice gap 0.2 mm, matrix 300 × 189, field of view 150 mm, flip

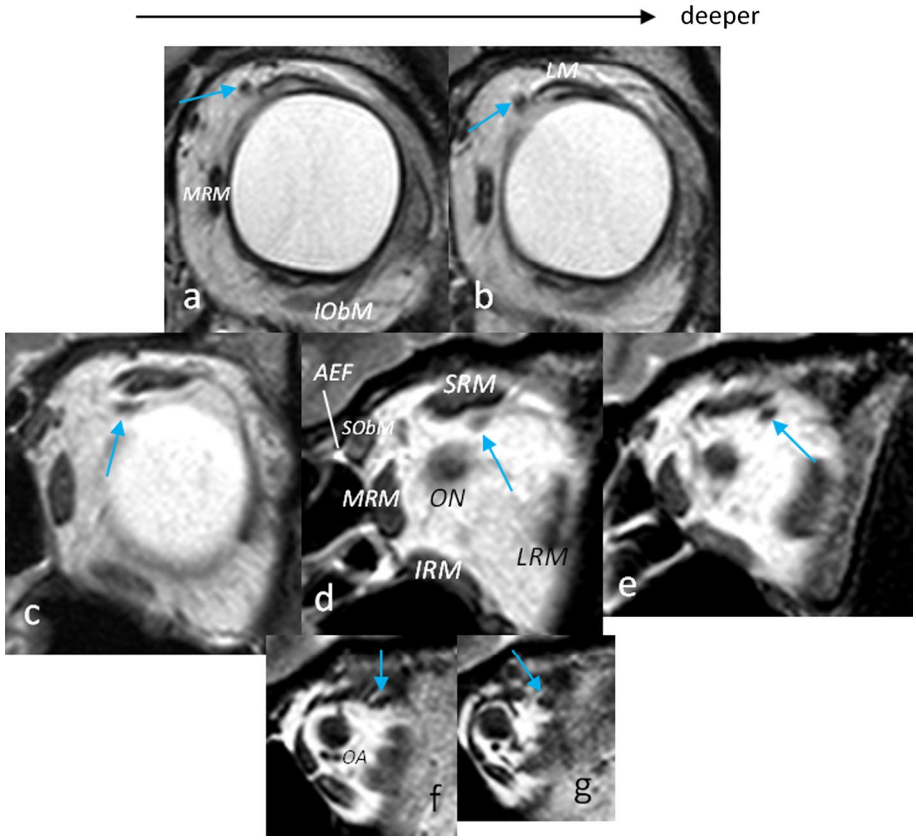

Fig. 2 Serial coronal T2-weighted magnetic resonance (MR) images of the same subject showing the supramuscular (**a**, **b**), inframuscular (**c**–**e**), and SOF segments (**f**, **g**) of the SOV. *AEF* Anterior ethmoidal foramen

angle 90º, and scan duration 6 min 40 s. 3D PC MR angiography was performed in the other 201 patients to delineate the SOV using the following parameters: TR 8.91 ms, TE 4.52 ms, slice thickness 0.3 mm, 100 frames, slab thickness 30 mm, matrix 256 × 256, field of view 100 mm, flip angle 10º, and scan duration 6 min 50 s. Velocity of blood flow encoding 10 or 20 cm/s was chosen for better visualization in all patients. MR imaging with intravenous gadolinium infusion (0.1 mmol/kg) was performed for 25 patients (12.4 %) who had tumorous lesions in the brain and skull. The basal image parallel to the anteroposterior dimension of the SOV was extracted from the individual imaging data as the representative image for analysis. All imaging data were transferred to a workstation (VirtualPlace Lexus64; AZE, Tokyo, Japan) and analyzed independently by two neurosurgeons (ST and YY).

Results

Coronal T2-weighted imaging

The 51 male and 50 female subjects who underwent coronal T2-weighted imaging were aged 12–81 years (mean 53 years). The intraorbital course of the SOV was clearly delineated on serial images in all patients. The SOV was topographically divided based on the relationship with the superior rectus muscle (SRM) into the supramuscular, inframuscular, and SOF segments (Fig. 2). The supramuscular segment of the SOV coursed extraconally in the posterolateral direction from the origin behind the tendon of the SObM to the medial edge of the SRM. The inframuscular segment corresponded to the part of the SOV coursing in the posterolateral direction along the lower surface of the SRM, above the optic nerve, as far as the lateral margin of the SRM. More distally, the SOF segment again coursed extraconally toward to the lateral part of the SOF. The SOV crossed over the ON at the level of the anterior ethmoidal foramina (AEF) in 87 % of right orbits and 71 % of left orbits (Fig. 3). The mean outer diameter of the SOV at the crossing point was 1.7 mm (range 0.4–4.6 mm) in the right orbit and 1.7 mm (range 0.4–4.1 mm) in the left orbit. The outer diameter showed a difference of more than 0.2 mm between sides in 76 subjects (75 %), larger in the right orbit in 40 (40 %) and larger in the left orbit in 36 (36 %). The maximum difference was 3.4 mm (right 4.6 mm, left 1.2 mm) found in a 36-year-old male.

3D PC MR angiography

The 99 male and 102 female subjects who underwent 3D PC MR angiography were aged 10–80 years (mean

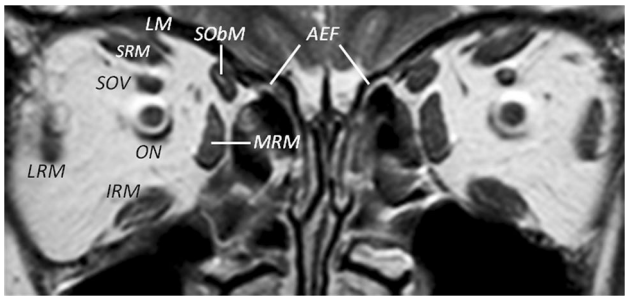

Fig. 3 Coronal T2-weighted MR image at the level of the AEF demonstrating the SOV located between the SRM and the ON

48 years). Delineation of the SOV showed considerable diversity (Fig. 4). The SOV was delineated in 96 patients (48 %), symmetrical in 32 (16 %), larger in the right orbit in 37 (18 %), and larger in the left orbit in 27 (13 %), and were unidentified in 105 (52 %) (Fig. 5). The SOV consistently coursed laterally to the ophthalmic artery (OA) in all patients. The entire course of the intraorbital SOV was identifiable in 47 % of subjects even without contrast agent, and was confirmed in 49 % on postcontrast images. Overall, administration of contrast agent did not significantly improve the delineation of the SOV, although resolution of the SOV tended to be better on postcontrast images (Fig. 4).

Discussion

The present study found common asymmetrical outer diameters in the bilateral SOVs, whereas the morphology entirely coursing lateral to the OA was highly consistent. Our series did not include infrequent anatomical variants of the OA [11, 12], which may attribute to the constant result. In more than 70 %, the SOV crossed over the ON at the level of the AEF on the coronal view, where the SRM, SOV, and ON were arranged in line vertically. We adopted the T2-weighted sequence because of its advantages, compared to the T1-weighted, fluid-attenuated inversion recovery, and fat-suppression sequences, for discriminating the SOV from other neurovascular structures lying in the orbital fat. As most of the orbital neurovascular and muscular structures are buried in the fat tissue, the AEF and anterior ethmoidal artery (AEA) passing through the AEF, which commonly identifiable from the superior direction, can be useful extraorbital landmarks during transcranial orbital surgery. The AEA, after arising from the intraorbital OA, passes through the AEF at the lamina papyracea of the medial orbital wall into the ethmoid air cells and cribriform plate, then turns superiorly to become the anterior falx artery [20].

Previously, the detection rate of the SOV was reported as 28 % by CT [1], 28.6−37.5 % by PC MR venography [6], and 26 % by carotid angiography [15]. The present study detected the SOV at 100 % by coronal T2-weighted MR imaging and 48 % by PC MR angiography, which were much higher rates. Therefore, we recommend these methods as useful, even without contrast agent, for visualizing the 3D architecture of the SOV in relation to the orbital neuromuscular structures.

In the present study, the mean outer diameter of the SOV at the crossing point over the ON showed prominent interindividual diversity and intraindividual asymmetry. The SOV also displayed common bilateral asymmetry on 3D PC angiography. Such findings may imply that apparently ectatic SOV found on neuroimaging does not necessarily suggest pathological conditions in the absence of clinical

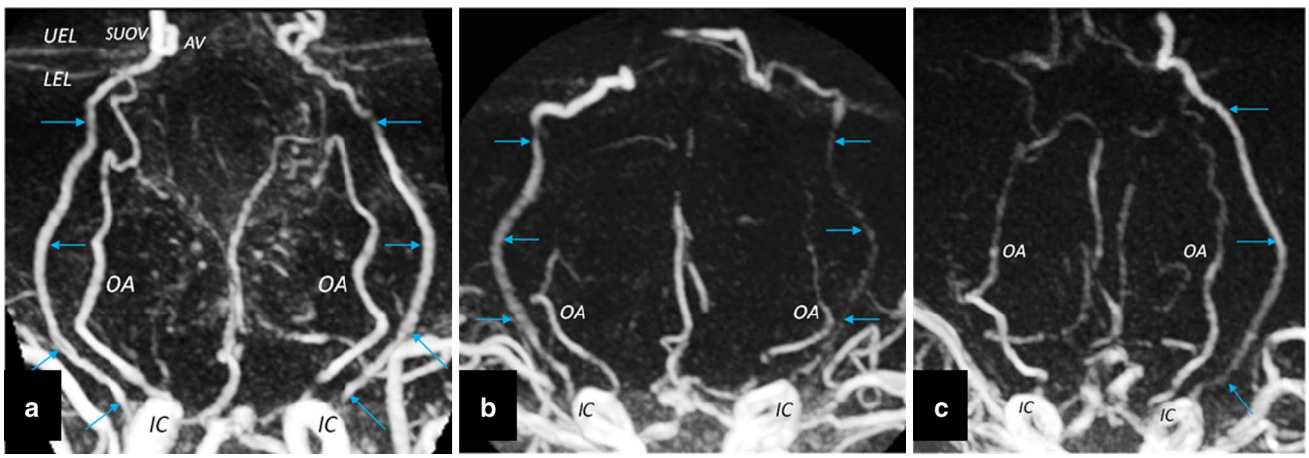

Fig. 4 Phase-contrast MR angiograms with (**a**) and without contrast agent (**b**, **c**) showing variable delineation of the SOVs (**a**–**c**, *arrows*) as symmetrical (**a**), larger in the right orbit (**b**), and larger in the left orbit (**c**). *AV* Angular vein, *IC* Internal carotid artery, *LEL* Lower eyelid, *SUOV* Supraorbital vein, *UEL* Upper eyelid

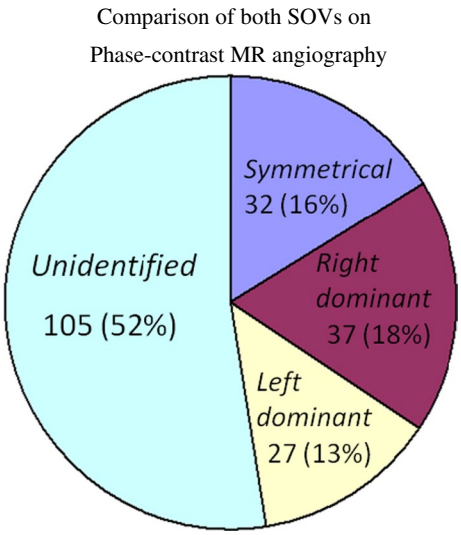

Fig. 5 Comparison of bilateral SOVs on 3D PC MR angiography

symptoms. A recent investigation suggested that the SOV, angular vein, and supraorbital vein may possess anatomically evident valves [23]. SOV diameter showed significant increase in the setting of increased intracranial pressure [9] and collapse in spontaneous intracranial hypotension [4]. A large bias of the size of SOV is probably induced by diverse factors that can influence the diameter of it. Further investigation is needed to discover whether such valves in the SOV and its tributaries function under physiological and pathological conditions and affect the luminal blood pressure and vessel diameter.

The present study has several limitations and defaults. Initially, our investigation was intended to delineate the SOV under physiological conditions, but some of our patients had clinical symptoms such as headache, dizziness, vertigo, seizure, and tinnitus. Therefore, unrecognized or underestimated pathological conditions might have influenced the outcome. Second, the present study was a retrospective trial, so selection bias may have affected the outcome. Third, velocity of blood flow encoding of 10 or 20 cm/s was chosen for each patient in the 3D PC MR angiography. We adopted these values for better delineation, compared to others, for both the SOV and OA, which was advantageous for understanding the spatial relationship between these vessels. Optimized values for individual SOVs might have improved the detection rate of the SOV.

Conclusions

The SOV consistently courses lateral to the OA but shows common bilateral asymmetry in outer diameter. The intraorbital course of the SOV can be divided into supramuscular, inframuscular, and SOV segments on the basis of topographical differences and the relationship with the SRM. The SRM, AEF, and AEA coursing in the AEF are valuable landmarks to identify the SOV lying in the orbital fat during transcranial orbital surgery. Combination of high-resolution MR imaging and 3D PC MR angiography is useful for delineating the SOV.

Conflict of interest The authors declare no conflict of interest concerning the materials or methods used in this study or the findings specified in this paper.

References

1. Bacon KT, Duchesneau PM, Weinstein MA (1977) Demonstration of the superior ophthalmic vein by high resolution computed tomography. Radiology 124:129–131
2. Brismar J (1974) Orbital phlebography. II. Anatomy of superior ophthalmic vein and its tributaries. Acta Radiol Diagn (Stockh) 15:481–496
3. Cellerini M, Mascalchi M, Mangiafico S, Ferrito GP, Scardigli V, Pellicanò G, Quilici N (1999) Phase-contrast MR angiography of intracranial dural arteriovenous fistulae. Neuroradiology 41:487–492
4. Chen WT, Fuh JL, Lirng JF, Lu SR, Wu ZA, Wang SJ (2003) Collapsed superior ophthalmic veins in patients with spontaneous intracranial hypotension. Neurology 61:1265–1267
5. Doyon DL, Aron-Rosa DS, Ramee A (1974) Orbital veins and cavernous sinus. In: Newton TH, Potts DG (eds) Radiology of the skull, chapter 76. Mosby, St Louis, pp 2220–2254
6. Ikawa F, Sumida M, Uozumi T, Kiya K, Kurisu K, Arita K, Satoh H (1995) Demonstration of the venous systems with gadolinium-enhanced three-dimensional phase-contrast MR venography. Neurosurg Rev 18:101–107
7. Ikawa F, Uozumi T, Kiya K, Kurisu K, Arita K, Sumida M (1996) Diagnosis of carotid-cavernous fistulas with magnetic resonance angiography–demonstrating the draining veins utilizing 3-D time-of-flight and 3-D phase-contrast techniques. Neurosurg Rev 19:7–12
8. Kurata A, Suzuki S, Iwamoto K, Miyazaki T, Inukai M, Abe K, Niki J, Yamada M, Fujii K, Kan S (2009) Direct-puncture approach to the extraconal portion of the superior ophthalmic vein for carotid cavernous fistulae. Neuroradiology 51:755–759
9. Lirng JF, Fuh JL, Wu ZA, Lu SR, Wang SJ (2003) Diameter of the superior ophthalmic vein in relation to intracranial pressure. AJNR Am J Neuroradiol 24:700–703
10. Natori Y, Rhoton AL Jr (1996) Microsurgical anatomy of the superior orbital fissure. Neurosurgery 36:762–775
11. N'da HA, Peltier J, Zunon-Kipré Y, Alsaiari S, Foulon P, Legards D, Havet E (2014) An unusual superolateral origin of ophthalmic artery: an anatomic case report. Surg Radiol Anat 36:95–97
12. Partlato C, di Nuzzo G, Luongo M, Tortora F, Briganti F (2011) Anatomical variant of origin of ophthalmic artery: case report. Surg Radiol Anat 33:275–278
13. Reis CV, Gonzalez FL, Zabramski JM, Hassan A, Deshmukh P, Albuquerque FC, Preul MC (2009) Anatomy of the superior ophthalmic vein approach for direct endovascular access to vascular lesions of the orbit and cavernous sinus. Neurosurgery 64(5 Suppl 2):318–323
14. Rohr AC, Riedel C, Fruehauf MC, van Baalen A, Bartsch T, Hedderich J, Alfke K, Doerner L, Jansen O (2011) MR imaging findings in patients with secondary intracranial hypertension. AJNR Am J Neuroradiol 32:1021–1029

15. Servo A (1982) Visualization of the superior ophthalmic vein on carotid angiography. Neuroradiology 23:141–146
16. Servo A, Jääskinen J (1983) The superior ophthalmic vein and tumours of the sellar area. Acta Neurochir (Wien) 68:195–202
17. Uchino A, Hasuo K, Matsumoto S, Masuda K (1992) MRI of dural carotid-cavernous fistulas. Comparisons with postcontrast CT. Clin Imaging 16:263–268
18. Vignaud J, Clay C, Aubin ML (1972) Orbital arteriography. Radiol Clin North Am 10:39–61
19. Weinstein MA, Modic MT, Risius B, Duchesneuan PM, Berlin AJ (1981) Visualization of the arteries, veins, and nerves of the orbit by sector computed tomography. Radiology 138:83–87
20. White DV, Sincoff EH, Abdulrauf SI (2005) Anterior ethmoidal artery: microsurgical anatomy and technical considerations. Neurosurgery 56(2 Suppl):406–410
21. Yousem DM, Atlas SW, Grossman RI, Sergott RC, Savino PJ, Bosley TM (1989) MR imaging of Tolosa-Hunt syndrome. AJNR Am J Neuroradiol 10:1181–1184
22. Yu SC, Cheng HK, Wong GK, Chan CM, Cheung JY, Poon WS (2007) Transvenous embolization of dural carotid-cavernous fistulae with transfacial catheterization through the superior ophthalmic vein. Neurosurgery 60:1032–1038
23. Zhang J, Stringer MD (2010) Ophthalmic and facial veins are not valveless. Clin Exp Ophthalmol 38:502–510